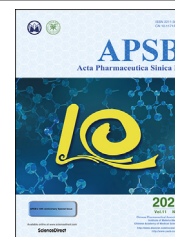




Chinese Pharmaceutical Association  
Institute of Materia Medica, Chinese Academy of Medical Sciences

Acta Pharmaceutica Sinica B

[www.elsevier.com/locate/apsb](http://www.elsevier.com/locate/apsb)  
[www.sciencedirect.com](http://www.sciencedirect.com)



ORIGINAL ARTICLE

# Mitochondrial protein IF1 is a potential regulator of glucagon-like peptide (GLP-1) secretion function of the mouse intestine



Ying Wang<sup>a</sup>, Jiaojiao Zhang<sup>a</sup>, Xinyu Cao<sup>b</sup>, Yaya Guan<sup>a</sup>,  
Shuang Shen<sup>b</sup>, Genshen Zhong<sup>a</sup>, Xiwen Xiong<sup>c</sup>, Yanhong Xu<sup>b</sup>,  
Xiaoying Zhang<sup>b</sup>, Hui Wang<sup>a,\*</sup>, Jianping Ye<sup>b,d,\*</sup>

<sup>a</sup>Henan Key Laboratory of Immunology and Targeted Therapy, Henan Collaborative Innovation Center of Molecular Diagnosis and Laboratory Medicine, School of Laboratory Medicine, Xinxiang Medical University, Xinxiang 453003, China

<sup>b</sup>Shanghai Diabetes Institute, Shanghai Jiao Tong University Affiliated Sixth People's Hospital, Shanghai 201306, China

<sup>c</sup>School of Forensic Medicine, Xinxiang Medical University, Xinxiang 453003, China

<sup>d</sup>Central Laboratory, Shanghai Sixth People's Hospital East Campus, Shanghai Jiao Tong University, Shanghai 201306, China

Received 24 November 2020; received in revised form 19 December 2020; accepted 7 January 2021

## KEY WORDS

GLP-1;  
ATPIF1;  
ANT2;  
L-cells;  
Mitophagy;  
Microbiota;  
Glucose tolerance;  
Insulin resistance

**Abstract** IF1 (ATPIF1) is a nuclear DNA-encoded mitochondrial protein whose activity is inhibition of the  $F_1F_0$ -ATP synthase to control ATP production. IF1 activity remains unknown in the regulation of GLP-1 activity. In this study, IF1 was examined in the diet-induced obese mice using the gene knockout (*If1*-KO) mice. The mice gained more body weight on a high fat diet without a change in food intake. Insulin tolerance was impaired, but the oral glucose tolerance was improved through an increase in GLP-1 secretion. The KO mice exhibited an improved intestine structure, mitochondrial superstructure, enhanced mitophagy, reduced apoptosis and decreased adenine nucleotide translocase 2 (ANT2) protein in the intestinal epithelial cells together with preserved gut microbiota. The data suggest that GLP-1 secretion was enhanced in the obese *If1*-KO mice to preserve glucose tolerance through a signaling pathway of ANT2/mitochondria/L-cells/GLP-1/insulin. IF1 is a potential mitochondrial target for induction of GLP-1 secretion in L-cells.

\*Corresponding authors.

E-mail addresses: [yejianping@sjtu.edu.cn](mailto:yejianping@sjtu.edu.cn) (Jianping Ye), [wanghui@xxmu.edu.cn](mailto:wanghui@xxmu.edu.cn) (Hui Wang).

Peer review under responsibility of Chinese Pharmaceutical Association and Institute of Materia Medica, Chinese Academy of Medical Sciences.

<https://doi.org/10.1016/j.apsb.2021.02.002>

2211-3835 © 2021 Chinese Pharmaceutical Association and Institute of Materia Medica, Chinese Academy of Medical Sciences. Production and hosting by Elsevier B.V. This is an open access article under the CC BY-NC-ND license (<http://creativecommons.org/licenses/by-nc-nd/4.0/>).

## 1. Introduction

Obesity increases the risk of type 2 diabetes through induction of insulin resistance. It is generally accepted that insulin resistance is a result of energy surplus, especially over supply of glucose. However, the molecular mechanism by which energy surplus leads to insulin resistance remains elusive although several hypotheses have been well documented in the literature<sup>1,2</sup>. Glucose, fatty acids and amino acids are the major energy substrates for ATP production by mitochondria. The production is dependent on F<sub>1</sub>F<sub>0</sub>-ATP synthase (ATPase) in the complex V, which utilizes the energy of mitochondrial potential to phosphorylate ADP in the ATP production. The mitochondrial ATPase also hydrolyzes ATP in thShanghai, China). The seqe conditions of substrate or oxygen deficiency in the maintenance of the mitochondrial membrane potential<sup>3</sup>. The hydrolysis activity is important in the protection of cells from apoptosis in the respiration-deficient conditions<sup>4</sup>. The ATPase activities are controlled by the F<sub>1</sub>F<sub>0</sub>-ATP synthase inhibitory protein 1 (ATPIF1, IF1)<sup>3</sup>. Under IF1 inactivation, the ATPase activities are enhanced in the production as well as hydrolysis of ATP<sup>5</sup>. The increased ATP production may promote insulin secretion in the pancreatic  $\beta$ -cells and GLP-1 secretion in the intestinal L-cells according to the physiology of the endocrine cells<sup>6</sup>. The endocrine alterations may impact glucose metabolism through insulin and GLP-1. However, the possibility has not been tested yet *in vivo* using *If1*-KO mice. To address this issue, we examined glucose metabolism in the *If1*-KO mice in this study.

IF1 activity has been investigated in the fields of cancer and inflammation in the regulation of cell metabolism<sup>7,8</sup>. However, the IF1 activity remains to be established in the pathophysiology of obesity and type 2 diabetes<sup>3</sup>. IF1 is an nuclei-encoded protein widely expressed in all tissues with higher levels in the energy-demanding tissues, such as the heart and skeletal muscle<sup>9</sup>. In the mitochondria, IF1 activity is regulated by phosphorylation and dimerization. The unphosphorylated IF1 proteins make up a homodimer that is bound to F<sub>1</sub>F<sub>0</sub>-ATPase to inhibit the enzyme activity<sup>10</sup>. The phosphorylation is catalyzed by the protein kinase A (PKA) at the site of serine 39 leading to tetramer formation, which makes IF1 disassociation from F<sub>1</sub>F<sub>0</sub>-ATPase to end the inhibition<sup>11</sup>. It is expected that physical exercise induces the IF1 phosphorylation in the heart and skeletal muscle to increase ATP production to meet the increased energy demand. The adaptation stimulates glucose uptake and catabolism in the muscle cells to enhance the insulin sensitivity. Therefore, inactivation of IF1 may lead to improvement of insulin sensitivity in the peripheral tissues. However, the possibility remains to be tested in a transgenic model.

In this study, the *If1*-KO mice were fed on a high fat diet (HFD) to examine the impact of IF1 inactivation in the glucose metabolism. The KO mice gained more fat tissues for an extra increase in the body weight. Insulin sensitivity was decreased in the skeletal muscle with impaired insulin tolerance. However, the glucose tolerance was improved in the same condition in the KO mice. The mechanism was that glucose-induced insulin and GLP-1 secretion

were both enhanced in the KO mice. Cell apoptosis was reduced and mitophagy was enhanced in the KO mice intestine to account for the improved GLP-1 secretion. The reduction in mitochondrial ANT2 protein was responsible for the GLP-1 secretion in the KO mice.

## 2. Materials and methods

### 2.1. Generation of *If1*-KO mice and DIO mice

All animal procedures were approved by the Institutional Animal Care and Use Committee (IACUC) of the Shanghai Jiao Tong University, Shanghai, China. The IF1 (*Atpif1*) knockout mouse was generated in C57BL/6 mice with the CRISPR/Cas9 gene editing method with sgRNA PAM sequences targeting *Atpif1*: SgRNA-1 GCAGTCGGATAGCATGGATACGG and SgRNA-2 GGCTCC ACCAGCTTCTCGGATGG. For identification of *If1*<sup>-/-</sup> mice, PCR was conducted to amplify the *If1* gene using the forward primer 5'-CATCAGCCTTGGAAATTCTGC-3' and the reverse primer 5'-CTTCGTCTCGGACTCGGTAG-3'. The agarose electrophoresis was performed to determine the genotype, and the amplified PCR product was used in gene sequencing with ABI-3730XL to confirm the genotype. The IF1 protein was examined to confirm the gene knockout. The homozygous KO mice (*If1*<sup>-/-</sup>) were bred by crossing the heterozygous mice (*If1*<sup>+/-</sup>) and used in this study. The wild type littermates (*If1*<sup>+/+</sup>) were used in the control. The mouse housing environment includes a 12:12-h light–dark cycle, constant room temperature (22–24 °C), free access to water and diet. The mice were fed on chow diet (fat content  $\geq$ 4% in weight, P1101F-25, Shanghai Pluteng Biotechnology Co., Ltd., China) or the high fat diet (HFD, fat = 40% in kcal, D12108C, Jiangsu Synergy, China). HFD feeding was started at 8 weeks in age to generate the diet-induced obese (DIO) model. Age- and gender-matched wild type mice were used in the control for the *If1*-KO mice.

### 2.2. Body weight, body composition and food intake

Body weight of mice was measured weekly. The body composition was determined using the quantitative nuclear magnetic resonance (NMR) (Minispec Mn10 NMR scanner, Bruker, Milton, ON, Canada) in the conscious and unrestrained mice, which was placed individually in a small tube for the NMR analyzer with 1 min in the assay. Food intake was measured manually in the individually housed mouse on HFD. A mean value of daily food intake was determined for each mouse over 3 days. Unit of food intake was g/mouse/day.

### 2.3. Energy expenditure and physical activity

Energy metabolism was monitored in the mice after 4 weeks on HFD, using the 20-cage Promethion-C continuous, parallel metabolic phenotyping system (Sable Systems International, Las Vegas, USA). Mice were kept in the metabolic chamber

individually for 6 days. The oxygen consumption ( $VO_2$ ), carbon dioxide production ( $VCO_2$ ), spontaneous physical activity and food intake were recorded daily for 5 days. The data on day 5 were used in the calculation of energy expenditure (EE: kcal/kg/h) and physical activity. The calculation was performed with Eq. (1):

$$EE = [3.815 + 1.232 \times VCO_2 / VO_2] \times VO_2 \times 0.001^{12} \quad (1)$$

Energy expenditure data was normalized with the body lean mass.

#### 2.4. ITT and GTT

Intraperitoneal insulin tolerance test (ITT) was performed in mice (9 weeks on chow diet and 14 weeks on HFD) by peritoneal insulin injection (0.75 U/kg body weight, I9278, Sigma) after 8 h fasting<sup>13</sup>. In DIO mice, oral glucose tolerance test (OGTT) and intraperitoneal glucose tolerance test (ipGTT) were performed in the mice (12–16 weeks on HFD) by administration of glucose (2 g/kg body weight) after overnight fasting. Blood glucose was measured in the tail vein blood at 0, 15, 30, 60, 90 and 120 min using the Accu-CHEK Advantage Blood Glucose Meter (Accu-CHEK; Indianapolis, IN, USA). Data were expressed in blood glucose concentration (mmol/L).

#### 2.5. Western blotting (WB)

Tissues (liver, muscle and colon) were collected from the mice after 16 weeks on HFD and examined for insulin signaling, apoptosis and mitophagy. The whole cell lysates were prepared from the tissue in WB according to the protocols described elsewhere<sup>12</sup>. Antibodies to IF1 (ab110277), VDAC1 (ab14734), PINK1 (ab186303), parkin (ab77924), total OXPHOS rodent (ab110413), P62 (ab56416), MFN (ab57602),  $\beta$ -actin (ab8224) and GAPDH (ab7291) were obtained from Abcam (Cambridge, MA, USA). Antibodies to ATG7 (8558S), ANT2 (14671S), caspase 3 (9662S), cleaved caspase 3 (9664S), DRP1 (8570S), AKT (C67E7) and p-AKT (T308, C31E5E) were purchased from the Cell Signaling Technology (Boston, USA). GAPDH and  $\beta$ -actin were used as the internal controls. WB images were quantified with the ImageJ software, whose value is expressed by integrated optical density (IOD).

#### 2.6. Quantitative real time PCR (qRT-PCR)

The total RNA was extracted from the tissue using TRIzol™ reagent (15596026, ThermoFisher, USA) according to the manufacturer's protocols. The qRT-PCR assay was performed with a kit of TB Green® Premix Ex Taq™ II (Tli RNase H Plus, RR820W, TaKaRa, Nijihigashi, Kusatsu, Shiga, Japan) using the ABI-3730XL machine. The target mRNA was normalized to the ribosome 18S RNA of the endogenous control. Primers and probes were purchased from TaKaRa (RR820A, Japan). Sequence of GLP-1 (*Gcg*) primers include the forward 5'-TTACTTTGTGGCTGGATTGCTT-3', and reverse 5'-AGTGGCGTTTGTCTTCATTCA-3'. The primers of *Ifi* gene are forward: 5'-ACGGGCGCTGGCTCCATCC-3'; reverse: 5'-TGGCGTTCAATTTGCTTCTG-3'.

#### 2.7. Insulin and GLP-1 assay

Insulin and GLP-1 were tested in the plasma of ocular vein blood of mice at 16 weeks on HFD using a protocol described in a

previous study<sup>13</sup>. Plasma insulin was measured using an insulin ELISA Kit (90080, Crystal Chem, Downers Grove, USA). The blood for GLP-1 assay was collected with a heparin tubes containing dipeptidyl peptidase IV inhibitor (10  $\mu$ L/mL, D3572, Merck, USA), which was conducted at 15 min after the glucose administration. The active form of GLP-1 was measured with the GLP-1 ELISA Kit (E-EL-M0090c, Elabscience, Wuhan, China).

#### 2.8. Hematoxylin and eosin (H&E) staining and transmission electron microscopy

The fresh intestinal tissues were fixed in 4% paraformaldehyde for 24 h in the H&E staining, and the electron microscope fixative at 4 °C for 2 h in the electron microscopy study using a protocol described in a previous study<sup>13</sup>. The samples were prepared by the Wuhan Servicebio technology Co., Ltd., Wuhan, China.

#### 2.9. Restoration of ANT2 in primary intestinal epithelial cells (IECs)

Mixed primary IECs were prepared from the fresh colon tissue with a protocol modified from a published study<sup>14</sup>. The colon tissue distal to the ileocolic junction was collected, rinsed in 75% alcohol and PBS briefly, and cut into small pieces at 1–2 mm/piece. The tissue was digested with 0.4 mg/mL collagenase IV (C4-28, Merck, USA), and cultured in Dulbecco's modified Eagle's medium (DMEM, 25 mmol/L glucose) supplemented with 10% FBS, 2 mmol/L L-glutamine, penicillin, and streptomycin. Aliquots were plated on Matrigel-coated 24-well plates ( $1 \times 10^5$ /well) for apoptosis studies following incubation for 2 days at 37 °C and 5% CO<sub>2</sub>. The cells were infected with an adenovirus expressing mouse ANT2 to restore the ANT2 level in the KO cells. The virus density was  $5.42 \times 10^{10}$  PFU (plaque forming unit)/mL in the stock solution and infection was conducted at 100 IFU (infect formation unit)/cell in the experiment. The ANT2 protein was determined in the cells by WB to confirm the restoration. Apoptosis was induced in the cells 24 h following the treatment by carbonyl cyanide m-chlorophenyl hydrazine (CCCP, 100  $\mu$ mol/L, #B5003, APExBIO) for 2 h. Apoptosis was determined in the cells with the cleaved caspases 3 signal by WB.

#### 2.10. Gut microbiota assay

The test was conducted in the fresh fecal samples with the 16S ribosomal RNA protocols<sup>13</sup>. The bacterial 16S rRNA genes V3–V4 region was amplified using the forward primer 338F (5'-ACTCCTACGGGAGGCAGCA-3') and the reverse primer 806R (5'-GGACTACHVGGGTWTCTAAT-3') in PCR. After purification with Agencourt AMPure Beads (Beckman Coulter, Indianapolis, IN, USA), the PCR products were quantified using the PicoGreen dsDNA Assay Kit (Invitrogen, Carlsbad, CA, USA). Sequencing was performed using the Illumina MiSeq platform with MiSeq Reagent Kit v3 at Shanghai Personal Biotechnology Co., Ltd. (Shanghai, China). The sequencing data was processed with the Quantitative Insights Into Microbial Ecology (QIIME, v1.8.0) pipeline. The RDP classifier with a bootstrap cutoff of 50% was used to determine the taxonomical assignments of representative sequences.

### 2.11. Statistical analysis

One-way ANOVA was used in the statistical analysis of data derived *in vivo*. In the *in vitro* studies, all experiments were repeated at least three times with consistent results, and the data from representative experiments are presented. Two-tailed, unpaired Student's *t*-test was used in the analysis of *in vitro* data. ImageJ was used to obtain band signal of WB data. All data are presented in mean  $\pm$  standard deviation (SD). The sample size or data point is indicated in the figure legend. The significance levels are indicated as \* $P < 0.05$ , \*\* $P < 0.001$ , and \*\*\* $P < 0.001$ .

## 3. Results

### 3.1. *If1*-KO mice gains more fat tissue on HFD

Obesity was induced in the *If1*-KO mice with HFD feeding to test the mouse response to oversupply of dietary energy. The KO mice gained more body weight than the WT mice (Fig. 1A). In the female mice, the initial body weight was identical. The KO mice exhibited a higher gain in the body weight than WT mice, which was observed throughout the study. A difference in the fat accumulation contributed to the extra weight gain in the KO mice as the total body fat mass, epididymal fat pad, and liver size were all higher in the KO mice (Fig. 1B and C). Energy expenditure were examined using the rodent metabolic chamber. A reduction was observed in the *If1*-KO mice (Fig. 1D). A reduction in physical activity was observed at day- and night-times (Fig. 1E). Food intake was not significantly altered in the mice (data not shown). The male KO mice also gained more fat on HFD (Fig. 1F). These data suggest that inactivation of *If1* gene led to an increased risk of obesity in the *If1*-KO mice from a reduction in energy expenditure.

### 3.2. Glucose tolerance is improved in the *If1*-KO mice by enhanced insulin secretion

In the *If1*-KO mice, glucose metabolism was examined in several tests including the intraperitoneal glucose tolerance (IPGTT), insulin tolerance (IPITT) and insulin signaling tests. The KO mice exhibited an improved glucose tolerance. In the IPGTT assay, the blood glucose was elevated after intraperitoneal injection of glucose at 2 g/kg body weight. The elevation was significantly attenuated in the KO mice (Fig. 2A). Plasma insulin and c-peptide were examined to understand the mechanism of improved glucose tolerance. Both insulin and c-peptide were significantly higher in the KO mice (Fig. 2B and C). In the ITT assay, the decrease in blood glucose was significantly less in the KO mice (Fig. 2D). The insulin signaling pathway was examined in the skeletal muscle and liver tissues of KO mice with AKT (S309) phosphorylation to understand the insulin resistance. A decreased insulin signaling was observed in both tissues (Fig. 2E and F). The phenotype suggests that IPGTT was improved in the obese KO mice from an increased insulin secretion by the pancreas. However, insulin sensitivity was impaired in the skeletal muscle and liver of the KO mice.

### 3.3. Plasma GLP-1 is elevated in the *If1*-KO mice

Above data suggest that insulin secretion was reprogrammed in the *If1*-KO mice to preserve glucose metabolism in the presence of insulin resistance. GLP-1 is a gut hormone with an activity in the stimulation of insulin secretion, which is one of the pharmacological activities of GLP1- related drugs in the treatment of type 2 diabetes. GLP-1 activity was examined in the obese KO mice to investigate the mechanism of insulin response in several experiments. Oral glucose tolerance test (OGTT), by which glucose induces GLP-1 secretion from the intestine, was conducted to test

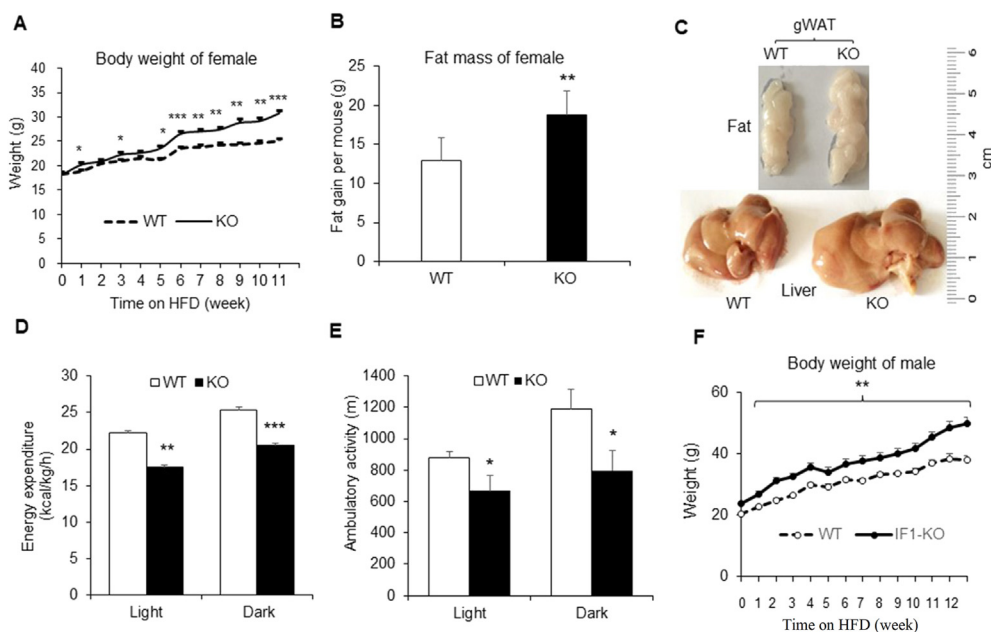


**Figure 1** Obesity was enhanced in the *If1*-KO mice. (A) Female mice body weight on HFD ( $n = 8-12$ ); (B) Fat mass of female mice on HFD ( $n = 9$ ); (C) Representative images of epididymal fat and liver of mice on HFD at 16 weeks on HFD; (D) Energy expenditure based on oxygen consumption rate in the female *If1*-KO mice after 4 weeks on HFD ( $n = 8$ ); (E) Physical ambulatory activity in the female *If1*-KO mice after 4 weeks on HFD ( $n = 8$ ); (F) Male mice body weight on HFD ( $n = 9$ ). The data represent mean  $\pm$  SD; \* $P < 0.05$ ; \*\* $P < 0.01$ , \*\*\* $P < 0.001$  vs. WT.

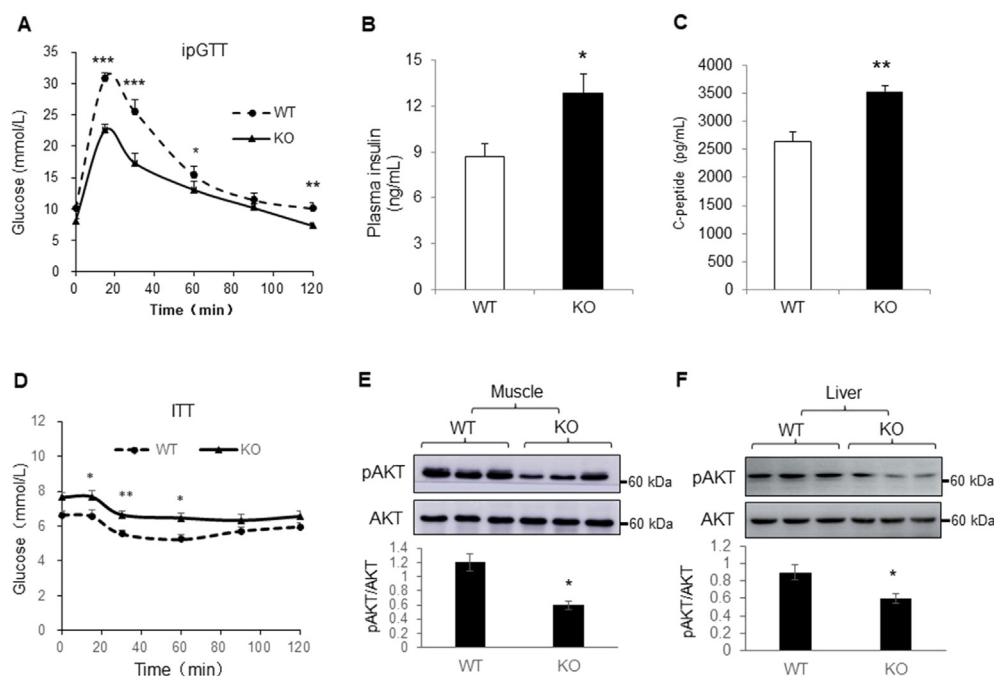


**Figure 2** Glucose tolerance is enhanced in the *Ifl*-KO mice. The female mice were subjected to the glucose tolerance test (GTT), insulin tolerance test (ITT), and insulin signaling test between 12 and 16 weeks on HFD. (A) IPGTT. The female mice were subjected to intraperitoneally glucose tolerance test (IPGTT) at dosage of 2 g/kg after overnight fasting at 12 weeks on HFD. The blood glucose was determined using the glucose meter at 5 time points ( $n = 8-12$ ). (B) Plasma insulin. Insulin was determined in the plasma at 15 min post glucose injection in the same mice at 13 weeks on HFD with ELISA assay ( $n = 5$ ). (C) Plasma c-peptide. The test was conducted with the same plasma of insulin test with the ELISA assay ( $n = 5$ ). (D) Intraperitoneal insulin tolerance test (IPITT). The same mice were injected with insulin (0.75 U/kg) intraperitoneally at 14 weeks on HFD after 8 h fasting. (E) Insulin signaling in muscle. The signal of pAKT (S308) was detected in the muscle of mice at 30 min after insulin injection at 16 weeks on HFD ( $n = 3$ ). (F) Insulin signaling in the liver. The test was conducted in the liver under the same condition as the muscle assay ( $n = 3$ ). The test was conducted in the liver under the same condition as the muscle assay ( $n = 3$ ). The experiment was repeated three times and representative blots are presented. The signal strength in the WB was quantified. The data represent mean  $\pm$  SD; \* $P < 0.05$ ; \*\* $P < 0.01$ , \*\*\* $P < 0.001$  vs. WT.

the GLP-1 secretion activity. OGTT was significantly improved in the *Ifl*-KO mice to support the possibility of GLP-1 alteration in the KO mice (Fig. 3A). Plasma GLP-1 level was examined after the oral glucose administration, and an increase was observed in the *Ifl*-KO mice (Fig. 3B). Expression of *Glp-1* mRNA was examined in the tissue of large intestine and a significant elevation was observed in the *Ifl*-KO mice (Fig. 3C). To exclude the impact of other tissue on the *Glp-1* expression, mRNA was examined in the primary culture of colon tissue and the increase was observed in the KO mice (Fig. 3D). The colon tissue histology was examined in the obese *Ifl*-KO mice to understand the mechanism of improved GLP-1 secretion. The tissue atrophy is a common change in the large intestine of DIO mice<sup>13</sup>. The atrophy was examined with H&E staining and a reduction in tissue atrophy was observed in the KO mice. The thickness of intestine wall was significantly higher in the *Ifl*-KO mice with abundant smooth muscle and mucosal layer (Fig. 3E and F). These data suggest that GLP-1 secretion was improved in the large intestine of obese *Ifl*-KO mice as result of resistance to tissue atrophy, which is consistent with the enhanced insulin secretion in the obese *Ifl*-KO mice for the improved glucose tolerance.

### 3.4. Intestinal epithelial cells are resistant to apoptosis in *Ifl*-KO mice

Apoptosis and mitochondrial structure were examined in the large intestine of KO mice to investigate the mechanism of anti-atrophy

phenotype. This was done in three experiments. The mitochondrial super structure was examined in the colonic epithelial cells under the transmission electron microscope. The cells have villi at the edge of the cavity side. The villi were healthier in the *Ifl*-KO mice with persistent length versus the sickness type of villi at different length in the WT mice (Fig. 4A). The epithelial cells of KO mice exhibited a difference from the KO mice in mitochondria in terms of size and matrix density. The KO cells had a smaller mitochondrion in general, and the mitochondria exhibited a higher matrix density (Fig. 4A), which are signs of healthy mitochondria. In contrast, the mitochondria of WT mice had a larger size and lower density of the mitochondrial matrix, in which the crista number was reduced. These are signs of damaged or old mitochondria. Apoptosis was examined in the large intestine tissue with the classical apoptosis marker, cleaved caspase 3 (c-caspase 3). The signal was detected in both KO and WT mice, while the signal was significantly reduced in the KO mice (Fig. 4B). The data suggest that the epithelial cells are more resistant to apoptosis in the KO mice with an improvement in mitochondria quality.

In search for the mechanism for the reduced apoptosis, we screened several mitochondrial proteins. One of the proteins, adenine nucleotide translocase 2 (ANT2), was reduced in the KO mice. ANT2 is an ADP/ATP translocase in the mitochondrial inner membrane, which contributes to apoptosis by mediating proton leak to induce collapse of mitochondrial potential<sup>15</sup>. A decrease in ANT2 activity leads to less proton leak in the suppression of cell apoptosis<sup>16,17</sup>. ANT2 protein was significantly

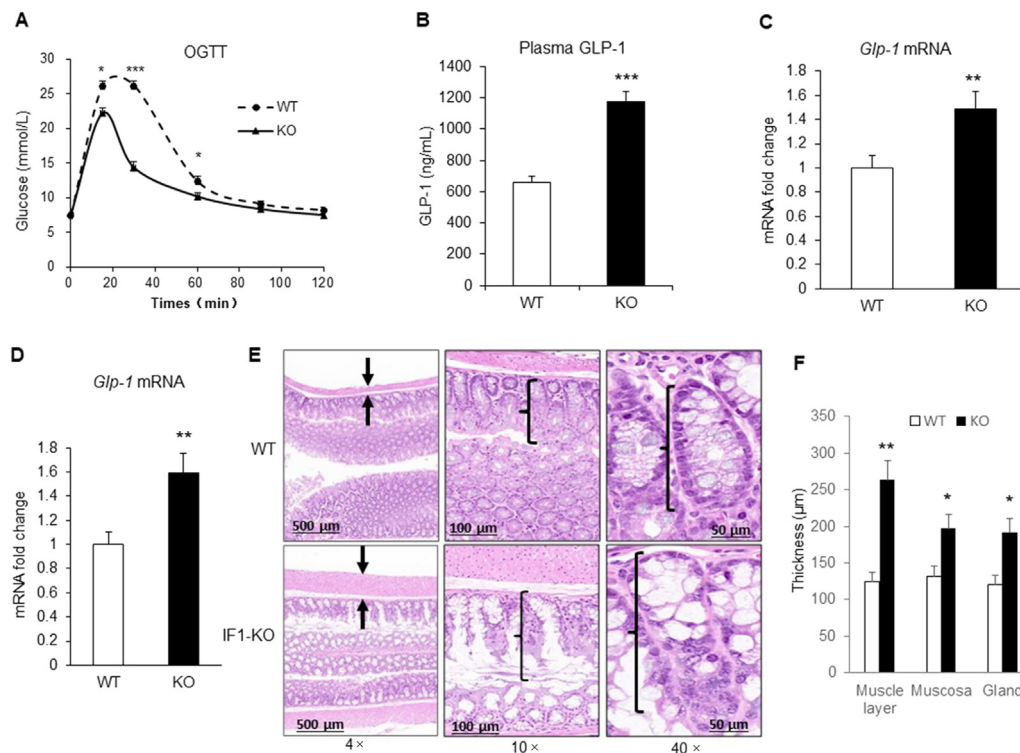


**Figure 3** GLP-1 secretion is increased in the *Ifl*-KO mice. (A) Oral glucose tolerance test (OGTT). The test was conducted in the mice after overnight fasting at 15 weeks on HFD by oral administration of glucose (2 g/kg) ( $n = 8-12$ ); (B) Plasma GLP-1 level. The test was conducted at 15 min post oral glucose administration using an enzyme-linked immunosorbent assay kit ( $n = 5$ ,  $P = 0.001$ ); (C) *Glp-1* mRNA in the colon tissue. mRNA was determined by qRT-PCR in the colon tissue of mice at 16 weeks on HFD ( $n = 6$ ); (D) *Glp-1* mRNA in the primary intestine culture. The primary culture of the large intestine was prepared, and mRNA of *Glp-1* was determined in the tissue by qRT-PCR after 24 h culture. (E) Reduced atrophy in the colon. The colon tissue slide was subjected to H&E staining and observed under the microscope. The tissue thickness is indicated by the arrows or markers. (F) Quantification of the intestine wall. The thickness of intestine wall was quantified in the H&E tissue slide and the results were expressed in the bar figure ( $n = 3$ ). The data represent mean  $\pm$  SD; \* $P < 0.05$ ; \*\* $P < 0.01$ ; \*\*\* $P < 0.001$  vs. WT.

reduced in the colon tissue of *Ifl*-KO mice (Fig. 4C). ANTI protein was not significantly altered (Fig. 4D). These data suggest that the reduction in ANTI2 may contribute to the reduction of apoptosis in the KO cells. To test the possibility, we expressed a recombinant *Ant2* gene to restore the ANTI2 protein level in the intestinal cells of the KO cells (Fig. 4E). The restoration resumed the apoptosis response in the KO cells (Fig. 4E). The data suggest that ANTI2 reduction is responsible for the decreased apoptosis in the KO mice.

### 3.5. Mitophagy is enhanced in the intestine of KO mice

The mechanism of ANTI2 reduction was investigated in the KO mice by examining mitophagy. Mitophagy is a mitochondria-specific autophagy response, which is induced by energy deficiency to recycle the damaged mitochondria to obtain energy substrate. Mitophagy controls mitochondrial quality to inhibit apoptosis<sup>18,19</sup>. The representative mitophagy protein markers, PINK1 and Parkin, were examined to determine the mitophagy activity of intestine tissues of the KO mice. Both signals were increased in the colon of *Ifl*-KO mice (Fig. 5A). Other representative proteins (P62 and AGT7) in the autophagy pathway were not significantly elevated in the same condition. The mitophagy activity was observed with more mitochondria in the autophagosome in the KO mice observed under the transmission electron microscope (Fig. 5B). The mitochondria are indicated by the white

color arrows in the autophagosome in the picture. The fusion and fission activities were examined in the mitochondria with the representative marker proteins, MFN1 and DRP1 (Fig. 5C). The respiratory chain was examined with the representative proteins (Fig. 5D). No significant change was observed in those markers in the KO mice. These data suggest that mitophagy was increased in the KO mice to improve the mitochondria quality control, which may provide a mechanism for the ANTI2 protein reduction in the large intestine of KO mice.

### 3.6. Gut microbiota is preserved in the large intestine of KO mice

The intestine function is influenced by the gut microbiota, which regulates the intestine integrity and endocrine function through several approaches. It is not known if the microbiota is altered in the *Ifl*-KO mice. To address this issue, we examined the microbiota in the fresh fecal samples of the mice on HFD. The microbiota diversity (richness and evenness) is increased in ACE index in DIO mice to count for the obesity-associated metabolic disorder. This diversity was reduced in the KO mice (Fig. 6A). Firmicutes and Bacteroidetes are the most abundant bacteria at the phylum level. The increase in Firmicutes and decrease in Bacteroidetes are the features in the wildtype obese mice. However, these changes were attenuated in the obese KO mice (Fig. 6B and C). The gut dysbiosis marker, the ratio of Firmicutes to

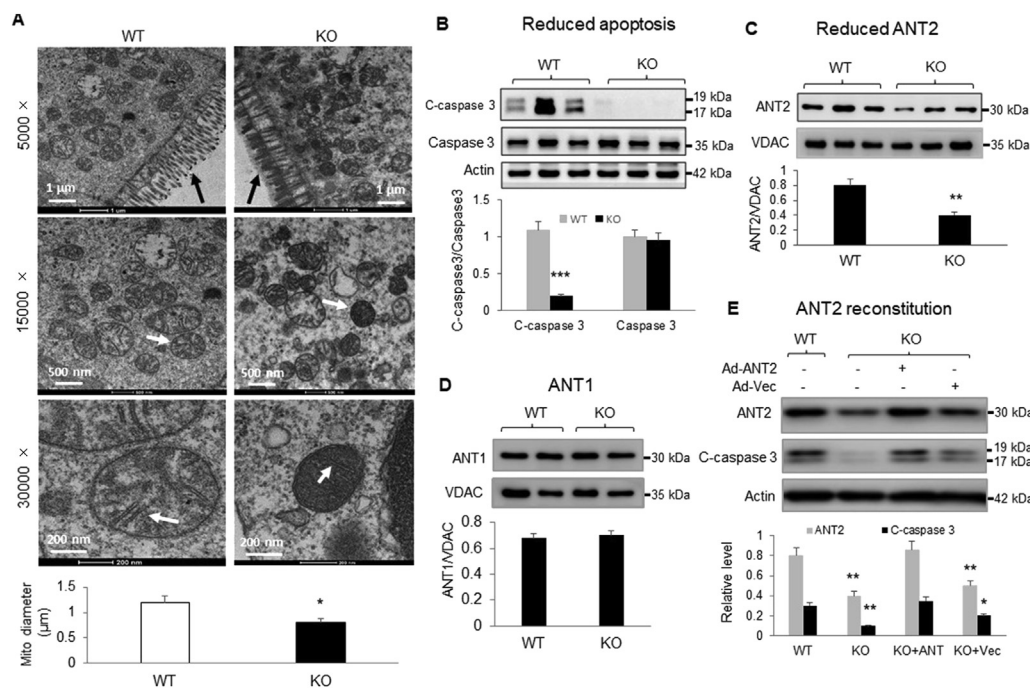


**Figure 4** Apoptosis of epithelial cells in *Ifl*-KO mice. (A) Transmission electronic microscope image. Mitochondria and villi were observed under the electronic microscope. The colon tissue was collected from the mice on HFD at 16 weeks and examined under the transmission electronic microscope. The mitochondrial diameter was quantified, and the results are expressed in the bar figure ( $n = 30$ ). (B) Cell apoptosis was reduced in the colon tissue of *Ifl*-KO mice. The representative proteins of apoptosis markers were examined by WB. (C) ANT2 protein. The protein was determined in the colon tissues (D) ANT1 protein. The protein was determined in the colon tissue by WB. (E) ANT2 reconstitution. Primary colon cells were collected from the colon of KO mice and tested in the cell culture. ANT2 was restored in the KO cells by expression of recombinant ANT2 delivered by adenovirus and the apoptosis was examined after CCCP treatment for 2 h. The bar figure presents data of mean  $\pm$  SD,  $n = 3$ ; \* $P < 0.05$ , \*\* $P < 0.01$  and \*\*\* $P < 0.001$  vs. WT.

Bacteroidetes, was increased in the wildtype DIO mice. The increase was attenuated in the KO mice (Fig. 6D). At the genus level, the butyrate-producing bacteria, Lachnospiraceae, was reduced in the KO mice (Fig. 6E). The data suggest that the microbiota is preserved in the KO mice to contribute to the gut function alteration.

#### 4. Discussion

Our study reveals that IF1 inactivation led to a reduction in energy metabolism in the KO mice for an increased risk of obesity. The *Ifl*-KO mice gained more adipose tissue on HFD, which was observed with two major changes. The first was reduction in the locomotion activity in the *Ifl*-KO mice for the less energy expenditure as indicated by the fall in oxygen consumption in the metabolic chamber. The reduction did not lead to a decrease in the food intake in *Ifl*-KO mice. The second was an enhancement of adipocyte differentiation that was observed *in vitro* in pre-adipocytes of the *Ifl*-KO mice<sup>20</sup>. Consistently, the obesity phenotype is in line with the observations in the *Ifl* overexpression mice, in which ROS production is enhanced<sup>21</sup> and inflammatory response is elevated<sup>22</sup>. ROS and inflammation promote energy expenditure in favor of suppression of obesity<sup>23</sup>. These studies suggest that IF1 may promote energy metabolism in the physiological condition to reduce the risk of obesity. Current study provides a substantial piece of evidence to support a role of IF1 in obesity, in which persistent inhibition of IF1 activity increases the risk of obesity. The *Ifl*-KO mice were normal in the growth, and

development on the chow diet, which is consistent with the observation by Nakamura et al<sup>24</sup>.

This study suggests that *Ifl* gene inactivation disassociates glucose intolerance and insulin intolerance in obesity. *Ifl* gene inactivation improved glucose tolerance, but impaired insulin tolerance in the *Ifl*-KO mice. In the WT mice, obesity induces both glucose intolerance and insulin intolerance. However, this rule was broken in the *Ifl*-KO mice on HFD. The reason is that insulin secretion was enhanced in the KO mice. IF1 was reported to suppress insulin secretion in a  $\beta$ -cell line *in vitro*<sup>25</sup>. Current study provides *in vivo* data to support the IF1 effect with elevated insulin secretion in the *Ifl*-KO mice. Interestingly, insulin sensitivity was decreased in the peripheral tissues of the *Ifl*-KO mice, which might be a result of mitochondrial reprogramming in the skeletal muscle. During this study, one study reported that IF1 was secreted by the skeletal muscle and injection of recombinant IF1 protein improved insulin sensitivity of skeletal muscle<sup>26</sup>. This study together with ours suggest that IF1 may be required in the muscle for maintenance of insulin sensitivity. However, a recent study reported that induction of IF1 activity in muscle by muscle-specific IF1 overexpression led to insulin resistance in the skeletal muscle of transgenic mice through suppression of mitochondrial ATP synthase<sup>27</sup>. Although the IF1 activity remains to be determined for insulin resistance, the studies consistently suggest that IF1 inhibits insulin secretion in the control of glucose metabolism in mice.

This study uncovers the relationship of IF1 and GLP-1. GLP-1 homologous are effective medicines in the treatment of type 2 diabetes, suggesting that the patients lack the GLP-1 activities.

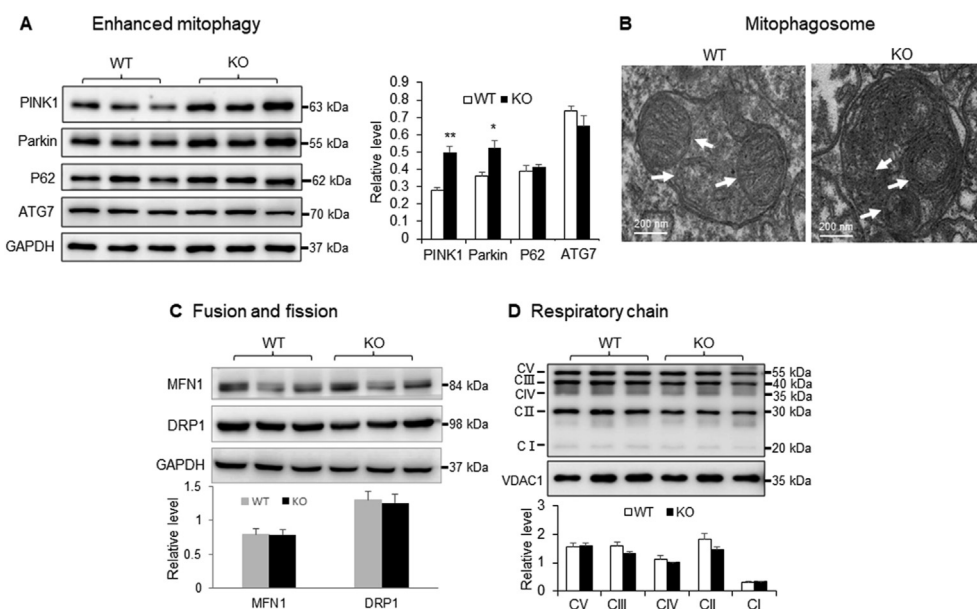


**Figure 5** Mitophagy in the large intestine of *Ifl*-KO mice. Mitophagy and autophagy activities were examined with marker proteins and autophagosomes in the large intestine of *Ifl*-KO mice on HFD at 16 weeks. (A) Mitophagy and autophagy markers in WB. (B) Autophagosomes observed under the transmission electronic microscope. (C) Mitochondrial fusion and fission markers in WB. (D) Respiratory chain protein in WB. Each experiment was repeated three times in this study and representative blot and image are presented. The signal strength in the WB was quantified. The results represent mean  $\pm$  SD,  $n = 3$ ; \* $P < 0.05$ , \*\* $P < 0.01$  vs. WT.

Induction of GLP-1 activity is a strategy in the treatment of type 2 diabetes. However, the ideal molecular targets remain elusive except DPP4 and GLP-1 receptor. We observed that GLP-1 activity was enhanced in the obese *Ifl*-KO mice, suggesting that IF1 is a potential target in the induction of GLP-1 secretion. This role of IF1 has not been reported in the literature. Regarding mechanism, the intestine of KO mice was resistant to atrophy. In obesity, GLP-1 is reduced by the atrophy of intestine tissue<sup>13</sup>, a tissue response to mitochondrial degeneration and cell apoptosis<sup>28</sup>. The apoptosis was reduced in the *Ifl*-KO mice, which is consistent with the observations in hepatocytes of the *Ifl*-KO liver<sup>29</sup>. However, in mechanism, we observed that mitochondrial structure was improved in the *Ifl*-KO cells for the reduced apoptosis. The observations suggest that IF1 may inhibit GLP-1 secretion in the physiological condition. Inhibition of IF1 activity may lead to an induction of GLP-1 secretion in the intestine.

The alteration in  $F_1F_0$ -ATPase activity may be a common mechanism for the phenotypes in multiple tissues of *Ifl*-KO mice. In the KO cells, the ATPase activity is enhanced in the production of ATP upon glucose challenge due to the absence of IF1. The increased ATP supply is a perfect mechanism for insulin secretion by  $\beta$ -cells and GLP-1 secretion by L-cells in the response to glucose<sup>30</sup>. ATP elevation is a common trigger for secretion of the two hormones<sup>6</sup>. In the energy deficient condition, the altered  $F_1F_0$ -ATPase activity leads to preservation of mitochondrial potential by consumption of ATP to reduce the risk of apoptosis through maintaining the mitochondrial potential.

Current study suggests a connection of IF1 and ANT2 in mitochondria. ANT2 is one of the three isoforms of ANT family of the ADP/ATP transporter proteins in mice<sup>31</sup>. ANTs import ADP from the cytoplasm into mitochondria, and export ATP from mitochondria to the cytoplasm<sup>32</sup>. In mice, ANT1 and ANT2 are expressed in all types of cells, ANT3 is not expressed and ANT4 expression is limited to the stem/germ cells<sup>31</sup>. ANT promotes

apoptosis through an interaction with the BCL family proteins<sup>15</sup>. However, the mechanism remains elusive until that ANT1 was found to mediate proton transportation cross the mitochondrial membrane in a study of the thermogenic activity of mitochondria<sup>33</sup>. An increase in the proton transportation leads to proton leak and mitochondrial potential collapse in favor of apoptosis<sup>16</sup>. In current study, the ANT2 (but not ANT1) protein was reduced in the *Ifl*-KO mice to count for the reduced apoptosis in the *Ifl*-KO mice. The mechanism by which ANT2 was reduced remains unclear. The ATP elevation may be a basis for the ANT2 protein reduction in the negative feedback regulation of ATP production, by which ADP supply is cut down in the mitochondria to reduce the ATP production. The possibility remains to be tested in experiment.

We observed that *Ifl* gene deletion enhanced mitophagy in the large intestine of *Ifl*-KO mice. Mitophagy controls mitochondrial quality by removal of the senescent and damaged mitochondria through self-digestion<sup>34</sup>, a process triggered by multiple factors including energy deficiency<sup>35</sup>. In current study, mitophagy was enhanced by IF1 inactivation in the *Ifl*-KO mice, which is consistent with the observations made by IF1 inhibition through shRNA-mediated gene knockdown<sup>21</sup> or gene knockout<sup>36</sup>. However, there is an opposite report that IF1 inhibition by gene knockdown led to reduction in mitophagy in a cellular model<sup>37</sup>. Induction of autophagy/mitophagy is in favor of energy metabolism as documented in reviews<sup>34,38</sup>. The mitophagy may be another mechanism for the ANT2 reduction in the KO mice. The relationship of mitophagy and ANT has recently been reported in a pharmacological study of ANT<sup>39</sup>. The gut microbiota profile was preserved in the intestine of obese KO mice, which may contribute to the mitophagy and cell apoptosis phenotypes in the KO mice. The exact signaling pathway remains to be investigated for the microbiota effect. The bile acid derivatives and sodium butyrate may involve in the signaling of microbiota<sup>40,41</sup>. The possibility remains to be tested by experiments.

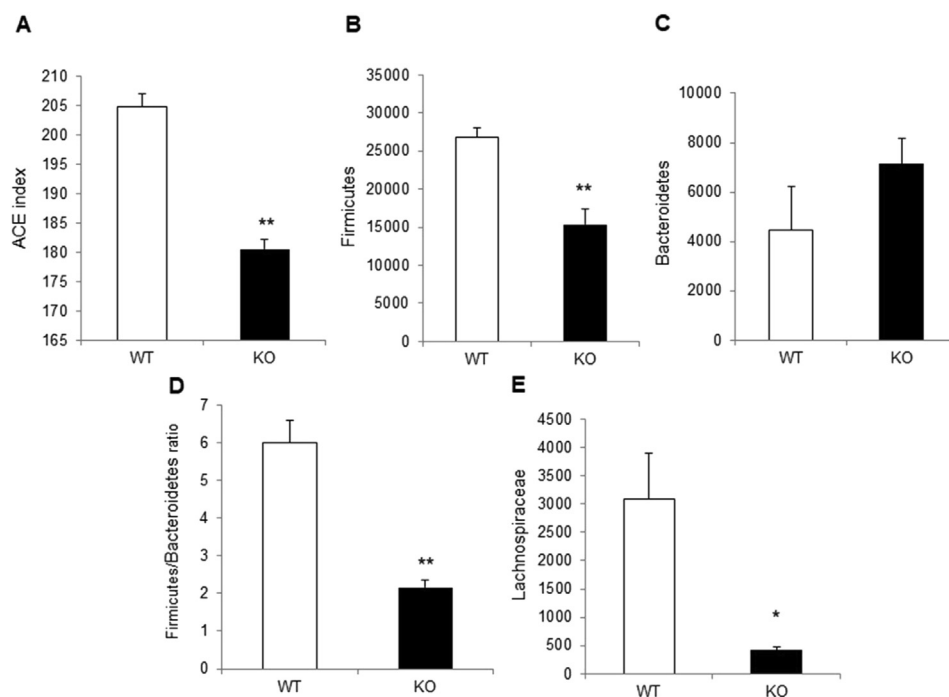


**Figure 6** Improved gut microbiota in the obese *Ifl*-KO mice. The fresh fecal samples were collected from the obese mice at 16 weeks on HFD and examined for gut microbiota. (A) Diversity of the microbiota. (B) Firmicutes. (C) Bacteroidetes. (D) Ratio of Firmicutes and Bacteroidetes. (E) Lachnospiraceae. The bar figure represents mean  $\pm$  SD,  $n = 5$ ; \* $P < 0.05$ , \*\* $P < 0.01$  vs. WT.

In summary, the role of *Ifl* gene was investigated in the pathogenesis of obesity in this study. The *Ifl*-KO mice exhibited a high risk of obesity with improved GTT, but impaired ITT on HFD. In the mechanism study, we found that the KO mice secreted more insulin and GLP-1 upon the glucose challenge. The large intestine was resistant to cell apoptosis and atrophy leading the enhanced GLP-1 secretion in the KO mice, which was associated with an improved mitochondrial structure in the intestinal epithelial cells. The reduced ANT2 protein was responsible for the apoptosis resistance. Mitophagy was enhanced to account for the improved mitochondrial quality. The microbiota profile was preserved in the large intestine of *Ifl*-KO mice on HFD, which may contribute to the intestinal phenotype in GLP-1 secretion. The elevated GLP-1 failed to improve insulin sensitivity and to inhibit obesity in the KO mice likely due to the direct effects of *Ifl*-KO on the insulin-sensitive tissues and brain.

### Acknowledgments

This study was funded by a project of the National Key Research and Development Program of China (2018YFA0800603) to Jianping Ye, the 111 Project (D20036, China) to Hui Wang, the National Natural Science Foundation-Henan Union grant of China (U1901131) to Genshen Zhong, the Training Program for Excellent Young Teachers in Higher Education of Henan Province (2017GGJS110, China) to Xiwen Xiong and the Health Commission of Henan Province (LHGJ20190497, China) to Yaya Guan.

### Author contributions

Ying Wang, Jiaojiao Zhang, Xinyu Cao, Yaya Guan, Shuang Shen, Genshen Zhong, Xiwen Xiong, Yanhong Xu and Xiaoying Zhang conducted the experiments, data analysis, figure preparation and

manuscript drafting. Hui Wang and Jianping Ye provided the concept, designed the study and edited the manuscript. All authors read and approved the final manuscript.

### Conflicts of interest

The authors declare no conflict of interest in publication of this study.

### References

- Roden M, Shulman GI. The integrative biology of type 2 diabetes. *Nature* 2019;**576**:51–60.
- Ye J. Mechanisms of insulin resistance in obesity. *Front Med* 2013;**7**:14–24.
- Cao X, Zhang X, Ye J. Regulation of mitochondrial atp synthase inhibitor 1 in cellular energy metabolism. *Chin J Cell Biol* 2020;**42**:682–90.
- Chen WW, Birsoy K, Mihaylova MM, Snitkin H, Stasinski I, Yucel B, et al. Inhibition of ATP1F1 ameliorates severe mitochondrial respiratory chain dysfunction in mammalian cells. *Cell Rep* 2014;**7**:27–34.
- Esparza-Molto PB, Nuevo-Tapioles C, Cuezva JM. Regulation of the  $H^+$ -ATP synthase by IF1: a role in mitohormesis. *Cell Mol Life Sci* 2017;**74**:2151–66.
- Muller TD, Finan B, Bloom SR, D'Alessio D, Drucker DJ, Flatt PR, et al. Glucagon-like peptide 1 (GLP-1). *Mol Metab* 2019;**30**:72–130.
- García-Aguilar A, Cuezva JM. A review of the inhibition of the mitochondrial ATP synthase by IF1 *in vivo*: reprogramming energy metabolism and inducing mitohormesis. *Front Physiol* 2018;**9**:1322.
- Esparza-Molto PB, Cuezva JM. The role of mitochondrial  $H^+$ -ATP synthase in cancer. *Front Oncol* 2018;**8**:53.
- Esparza-Molto PB, Nuevo-Tapioles C, Chamorro M, Najera L, Torresano L, Santacatterina F, et al. Tissue-specific expression and post-transcriptional regulation of the atpase inhibitory factor 1 (IF1) in human and mouse tissues. *Faseb J* 2019;**33**:1836–51.

10. Gu J, Zhang L, Zong S, Guo R, Liu T, Yi J, et al. Cryo-em structure of the mammalian ATP synthase tetramer bound with inhibitory protein if1. *Science* 2019;**364**:1068–75.
11. Garcia-Bermudez J, Sanchez-Arago M, Soldevilla B, Del Arco A, Nuevo-Tapióles C, Cuezva JM. PKA phosphorylates the atpase inhibitory factor 1 and inactivates its capacity to bind and inhibit the mitochondrial H<sup>+</sup>-ATP synthase. *Cell Rep* 2015;**12**:2143–55.
12. Ke B, Zhao Z, Ye X, Gao Z, Manganiello V, Wu B, et al. Inactivation of NF- $\kappa$ B p65 (RelA) in liver improved insulin sensitivity and inhibited cAMP/PKA pathway. *Diabetes* 2015;**64**:E496–505.
13. Le J, Zhang X, Jia W, Zhang Y, Luo J, Sun Y, et al. Regulation of microbiota–GLP1 axis by senoside a in diet-induced obese mice. *Acta Pharm Sin B* 2019;**9**:758–68.
14. Reimann F, Habib AM, Tolhurst G, Parker HE, Rogers GJ, Gribble FM. Glucose sensing in l cells: a primary cell study. *Cell Metabol* 2008;**8**:532–9.
15. Zhivotovsky B, Galluzzi L, Kepp O, Kroemer G. Adenine nucleotide translocase: a component of the phylogenetically conserved cell death machinery. *Cell Death Differ* 2009;**16**:1419–25.
16. Qin X, Xu Y, Peng S, Qian S, Zhang X, Shen S, et al. Sodium butyrate opens mitochondrial permeability transition pore (mPTP) to induce a proton leak in induction of cell apoptosis. *Biochem Biophys Res Commun* 2020;**527**:611–7.
17. Wu K, Luan G, Xu Y, Shen S, Qian S, Zhu Z, et al. Cigarette smoke extract increases mitochondrial membrane permeability through activation of adenine nucleotide translocator (ANT) in lung epithelial cells. *Biochem Biophys Res Commun* 2020;**525**:733–9.
18. Ham SJ, Lee D, Yoo H, Jun K, Shin H, Chung J. Decision between mitophagy and apoptosis by parkin via vdac1 ubiquitination. *Proc Natl Acad Sci U S A* 2020;**117**:4281–91.
19. Lin J, Zhuge J, Zheng X, Wu Y, Zhang Z, Xu T, et al. Urolithin A-induced mitophagy suppresses apoptosis and attenuates intervertebral disc degeneration via the AMPK signaling pathway. *Free Radic Biol Med* 2020;**150**:109–19.
20. Guan Y, Liang Y, Wang H, Ye J. Knockout of ATP synthase inhibitory factor 1 (ATPIF1) gene increased intracellular ATP level in primary fibroblast cells and promoted adipocyte differentiation. *J Xinxiang Med Coll* 2018;**35**:658–61.
21. Campanella M, Seraphim A, Abeti R, Casswell E, Echave P, Duchon MR. IF1, the endogenous regulator of the F<sub>1</sub>F<sub>0</sub>-ATP synthase, defines mitochondrial volume fraction in HeLa cells by regulating autophagy. *Biochim Biophys Acta* 2009;**1787**:393–401.
22. Formentini L, Sánchez-Aragó M, Sánchez-Cenizo L, Cuezva José M. The mitochondrial ATPase inhibitory factor 1 triggers a ros-mediated retrograde pro-survival and proliferative response. *Mol Cell* 2012;**45**:731–42.
23. Wang H, Ye J. Regulation of energy balance by inflammation: common theme in physiology and pathology. *Rev Endocr Metab Disord* 2015;**16**:47–54.
24. Nakamura J, Fujikawa M, Yoshida M. IF1, a natural inhibitor of mitochondrial ATP synthase, is not essential for the normal growth and breeding of mice. *Biosci Rep* 2013;**33**:735–41.
25. Kahancova A, Sklenar F, Jezek P, Dlaskova A. Regulation of glucose-stimulated insulin secretion by ATPase inhibitory factor 1 (IF1). *FEBS Lett* 2018;**592**:999–1009.
26. Lee HJ, Moon J, Chung I, Chung JH, Park C, Lee JO, et al. ATP synthase inhibitory factor 1 (IF1), a novel myokine, regulates glucose metabolism by AMPK and AKT dual pathways. *Faseb J* 2019;**33**:14825–40.
27. Sanchez-Gonzalez C, Nuevo-Tapióles C, Herrero Martin JC, Pereira MP, Serrano Sanz S, Ramirez de Molina A, et al. Dysfunctional oxidative phosphorylation shunts branched-chain amino acid catabolism onto lipogenesis in skeletal muscle. *EMBO J* 2020;**39**:e103812.
28. Sun Y, Jin C, Zhang X, Jia W, Le J, Ye J. Restoration of GLP-1 secretion by berberine is associated with protection of colon enterocytes from mitochondrial overheating in diet-induced obese mice. *Nutr Diabetes* 2018;**8**:53.
29. Faccenda D, Nakamura J, Gorini G, Dhoot GK, Piacentini M, Yoshida M, et al. Control of mitochondrial remodeling by the ATPase inhibitory factor 1 unveils a pro-survival relay via OPA1. *Cell Rep* 2017;**18**:1869–83.
30. Sun EW, de Fontgalland D, Rabbitt P, Hollington P, Sposito L, Due SL, et al. Mechanisms controlling glucose-induced GLP-1 secretion in human small intestine. *Diabetes* 2017;**66**:2144–9.
31. Rodic N, Oka M, Hamazaki T, Murawski MR, Jorgensen M, Maatouk DM, et al. DNA methylation is required for silencing of ANT4, an adenine nucleotide translocase selectively expressed in mouse embryonic stem cells and germ cells. *Stem Cell* 2005;**23**:1314–23.
32. Ruprecht JJ, King MS, Zogg T, Aleksandrova AA, Pardon E, Crichton PG, et al. The molecular mechanism of transport by the mitochondrial ADP/ATP carrier. *Cell* 2019;**176**:435–447 e15.
33. Bertholet AM, Chouchani ET, Kazak L, Angelin A, Fedorenko A, Long JZ, et al. H<sup>+</sup> transport is an integral function of the mitochondrial ADP/ATP carrier. *Nature* 2019;**571**:515–20.
34. Zhang Y, Sowers JR, Ren J. Targeting autophagy in obesity: from pathophysiology to management. *Nat Rev Endocrinol* 2018;**14**:356–76.
35. Wang L, Qi H, Tang Y, Shen HM. Post-translational modifications of key machinery in the control of mitophagy. *Trends Biochem Sci* 2019;**45**:58–75.
36. Yang K, Long Q, Saja K, Huang F, Pogwizd SM, Zhou L, et al. Knockout of the atpase inhibitory factor 1 protects the heart from pressure overload-induced cardiac hypertrophy. *Sci Rep* 2017;**7**:10501.
37. Lefebvre V, Du Q, Baird S, Ng AC, Nascimento M, Campanella M, et al. Genome-wide RNAi screen identifies ATPase inhibitory factor 1 (ATPIF1) as essential for PARK2 recruitment and mitophagy. *Autophagy* 2013;**9**:1770–9.
38. Rovira-Llopis S, Banuls C, Diaz-Morales N, Hernandez-Mijares A, Rocha M, Victor VM. Mitochondrial dynamics in type 2 diabetes: pathophysiological implications. *Redox Biol* 2017;**11**:637–45.
39. Hoshino A, Wang WJ, Wada S, McDermott-Roe C, Evans CS, Gosis B, et al. The ADP/ATP translocase drives mitophagy independent of nucleotide exchange. *Nature* 2019;**575**:375–9.
40. Gao Z, Yin J, Zhang J, Ward RE, Martin RJ, Lefevre M, et al. Butyrate improves insulin sensitivity and increases energy expenditure in mice. *Diabetes* 2009;**58**:1509–17.
41. Zheng X, Chen T, Jiang R, Zhao A, Wu Q, Kuang J, et al. Hyocholic acid species improve glucose homeostasis through a distinct TGR5 and FXR signaling mechanism. *Cell Metabol* 2020;**S1550**–4131:30652–5.